Article

Not peer-reviewed version

A New Record of *Antithamnion hubbsii* (Ceramiales, Rhodophyta) from the Korean Coast: Invasive Species Interactions with Native and Non-Native Communities

Eunyoung Shim , Soo Yeon Kim , Giuseppe C. Zuccarello , Gwang Hoon Kim *

Posted Date: 28 August 2025

doi: 10.20944/preprints202508.2023.v1

Keywords: *Antithamnion hubbsii*; red alga; Ceramiales; invasive species; Korean coast; *molecular phylogeny*; *rbc*L; *psa*A; species delimitation

 doi:10.20944/preprints202508.2023.v1

Article

A New Record of *Antithamnion hubbsii* (Ceramiales, Rhodophyta) from the Korean Coast: Invasive Species Interactions with Native and Non-Native Communities

Eunyoung Shim [1], Soo Yeon Kim [2], Giuseppe C. Zuccarello [3] and Gwang Hoon Kim [2,*]

[1] Biotechnology Research Institute, Kongju National University, Gongju, Republic of Korea
[2] Department of Biological Sciences, Kongju National University, Gongju 32588, Korea
[3] School of Biological Sciences, Victoria University of Wellington, P.O. Box 600, Wellington 6140, New Zealand
* Correspondence: ghkim@kongju.ac.kr

Abstract

Taxonomic clarity within the genus *Antithamnion* is important in the molecular phylogeny of red algae. *Antithamnion hubbsii* is reported for the first time from the Korean coast, previously misidentified as *A. nipponicum* due to morphological similarities. Specimens collected from Gangneung were analyzed using plastid-encoded *rbc*L and *psa*A genes, confirming their identity as *A. hubbsii*. Korean specimens exhibit indeterminate lateral axes, oppositely arranged pinnae and pinnules, and distinctive gland cells on the adaxial surface of pinnules. Molecular analyses revealed minimal genetic divergence between the two species (1-3 base pair differences in *rbc*L, none in *psa*A). While PTP analysis differentiated them as distinct species, ASAP and ABGD analyses grouped them as a single species. Despite these results, our phylogenetic analyses showed Korean *A. hubbsii* forming a distinct clade with strong bootstrap support. However, further research is needed to clarify the taxonomic boundaries between *A. hubbsii* and *A. nipponicum*. Our ecological observations revealed that this North American invasive species competes with both native red algal communities and established non-natives, apparently outcompeting *A. nipponicum* in shared habitats. This suggests potential shifts in community composition and ecological functions along the Korean coast as this invader spreads.

Keywords: *Antithamnion hubbsii;* red alga; Ceramiales; invasive species; Korean coast; molecular phylogeny; *rbc*L; *psa*A; species delimitation

1. Introduction

Marine ecosystems serve as habitats for various algal species, which play crucial roles as primary producers. Red algae (Rhodophyta) have adapted to diverse environments and are widely distributed throughout the world's oceans (Rueness et al., 2007). Among them, the genus *Antithamnion* has received continuous attention from marine biologists due to its morphological diversity and ecological significance. For instance, *Antithamnion nipponicum* has been introduced to new regions, such as the Norwegian coast, highlighting the impact of globalization on marine ecosystems (Rueness, 2007). Additionally, *Antithamnion sparsum* has been recently recorded in the Northwest Atlantic, showcasing the ongoing spread of non-indigenous species in marine environments (Brooks and Krumhansl, 2023).

The study by Cho et al. (2007) made significant contributions to resolving taxonomic confusion within the genus *Antithamnion*. Their research clarified the relationship between *A. hubbsii* and *A.*

 doi:10.20944/preprints202508.2023.v1

nipponicum while providing molecular evidence that *A. nipponicum* is distinct from *A. pectinatum*. However, later finds of a similar alga from the Azores (Athanasiadis & Tittley, 1994) were classified as *A. pectinatum* (Montagne) Brauner, with *A. nipponicum* reduced to synonymy (with a question mark), further illustrating the historical ambiguity surrounding these taxa. According to their findings, *A. hubbsii* and *A. nipponicum* have nearly identical *rbc*L gene sequences and share morphological characteristics, leading to the proposal that they may represent the same species. They confirmed the presence of *A. nipponicum* along the Pacific and Atlantic coasts of North America, suggesting it was a recent introduction from Japan.

However, misidentifications within the genus *Antithamnion* remain common due to the high degree of morphological similarity among species (Cho et al. 2007). In particular, *A. nipponicum* and *A. hubbsii* possess very similar morphological features, making them difficult to distinguish using traditional methods alone. Cho et al. emphasized that the key identifying features of *A. hubbsii* include indeterminate lateral axes of pinnae, oppositely arranged pinnules, and gland cells located on the adaxial surface of pinnules.

Until now, only *A. nipponicum* has been reported from Korean waters, with no confirmed presence of *A. hubbsii*. However, through detailed morphological observations and molecular phylogenetic studies of specimens collected from the eastern coast of Gangneung, it was revealed that some specimens previously identified as *A. nipponicum* are actually *A. hubbsii*. This represents the first report of *A. hubbsii* in Korean waters, deepening our understanding of red algal biodiversity in Korea.

The introduction pathway of marine invasive species is often linked to international maritime activities. In the case of *A. hubbsii* in Korean waters, two potential introduction vectors are worthy of investigation. First, given that *A. hubbsii* has been well-documented along the Pacific coast of North America (Cho et al., 2007), increasing cruise ship traffic between North American ports and Korean destinations could serve as a potential vector. Cruise ships carry large volumes of ballast water and provide hull surface area for biofouling organisms, both of which are recognized as major pathways for marine species introductions (Carlton & Geller, 1993). Second, considering that Japan is geographically proximate to Korea and that *A. nipponicum* is native to Japanese waters, natural dispersal or smaller-scale maritime activities between Japan and Korea could have facilitated the introduction of *A. hubbsii*, especially if it was previously misidentified in Japan as well.

Our research employs both traditional morphological and modern molecular approaches to accurately identify and characterize *A. hubbsii* from Korean waters. This integrated approach is essential for distinguishing between morphologically similar species and establishing the phylogenetic relationships between Korean specimens and those from other regions. By documenting this new record and investigating its introduction pathway and ecological context, this study contributes to our understanding of marine biodiversity in Korea and provides valuable information for monitoring and managing non-native species in Korean coastal ecosystems.

2. Materials and Methods

2.1. Sampling, Culture and Microscopy

The samples were collected in the rocky intertidal of Sungeut beach (37°49′2.6″N, 128°53′40.5″E), Gangneung-si, Gangwon-do, Korea, on January 6, 2024. Culture conditions consisted of sterilized seawater supplemented with IMR (Institute of Marine Resources) medium as described by Klochkova et al. (2006). Samples were maintained at 20°C under cool-white fluorescent lights providing >20 μmol photons m^{-2} s^{-1}, with a 16 h light/8 h dark cycle. Culture maintenance involved transfer to new IMR medium every 7-14 days. Samples including the type specimen were deposited at the National Marine Biodiversity Institute of Korea (MABIK: AL00100***).

Live imaging was performed using an Olympus BX54 research microscope featuring differential interference contrast (DIC) capabilities and integrated with a Samsung iPolis imaging system (Samsung, Suwon, Korea). Nuclear visualization was performed following cell fixation in culture media using microwave irradiation for a few seconds. Subsequently, cells were stained with Hoeschst

 doi:10.20944/preprints202508.2023.v1

33342 (1 µl/mL in the IMR medium) for 15 minutes under dark conditions prior to microscopic examination. Light and fluorescence microscopy images were merged using Adobe Photoshop CS6 software. The images were then analyzed using ImageJ software (NIH, http://imagej.nih.gov/ij/) to quantify the length of the cells and the diameter of the nuclei.

2.2. Molecular Analysis

Total DNA was extracted from fresh or dried samples using the Chelex method (Zuccarello et al. 1999). The partial sequence of the plastid-encoded ribulose-1, 5-bisphosphate carboxylase/oxygenase large subunit gene (*rbc*L) was amplified using the primer pairs F321 and R1150 (Kang et al. 2020). PCR conditions followed a touchdown PCR as follows: initial denaturation at 94°C for 4 min, followed by 10 cycles of 94°C for 1 min, 55°C for 30sec, and a decrease in annealing temperature by 1°C per cycle, and 72°C for 1 min; followed by 25 cycles of 94°C for 1min, 45°C for 30sec, and 72°C for 1 min and a final step at 72°C for 5 min. Additionally, the partial sequence of the plastid-encoded photosystem I P700 chlorophyll a apoprotein A1 gene (*psa*A) was amplified using the primer pairs *psa*A130F (5′-AACWACWACTTGGATTCGAA-3′) and *psa*A1760R (5′-CCTCTWCCWGGWCATCWCAWGG-3′) (Yoon et al. 2002; Saunders & Moore 2013). The PCR conditions for *psaA* followed a touchdown protocol: initial denaturation at 94°C for 2 min, followed by 5 cycles of 94°C for 30 s, 45°C for 30 s, and 72°C for 1 min; then 35 cycles of 94°C for 30 s, 46.5°C for 30 s, 72°C for 1 min, and a final extension at 72°C for 7 min. PCR products were purified using Zymoclean™ Gel DNA recovery Kit (Zymo Research, USA). PCR products were sent for commercial Sanger sequencing using both sets of PCR primers (Cosmogene Tech, Daejeon, Korea). Sequences were edited and assembled in Geneious® Prime 2025.1.2 (https://www.geneious.com).

For phylogenetic analyses, the newly determined *rbc*L and *psa*A sequences were analyzed alongside sequences from various *Antithamnion* and *Anthithamnionella* species, plus related genera downloaded from GenBank. Details of all specimens used in this study, including collection information, voucher numbers, and GenBank accession numbers, are presented in Table 1. The data set was aligned using MAFFT in Geneious® Prime 2025.1.2 (https://www.geneious.com) together with our new sequences of *Antithamnion hubbsii* collected from Korea (PV453999). Phylogenetic analyses were performed using the maximum likelihood (ML) method with IQ-TREE 2.3.4 (Minh et al. 2020). Codon positions were partitioned and the best-fit model was determined using ModelFinder (Kalyaanamoorthy et al. 2017) and partition model (Chernomor et al. 2016). The *rbc*L DNA substitution models were selected for each codon (i.e., first codon: TN+F+I; second codon: F81+F+I; third codon: HKY+F+G4) were selected. The *psa*A DNA substitution models were selected for each codon (i.e., first codon: TIM2+F+G4; second codon: TIM+F+I; third codon: TPM3u+F+I) were selected. Support for each internal branch was determined by non-parametric bootstrap (500 replicates) (Felsenstein 1985). Bayesian inference analysis was conducted with MrBayes v. 3.2 (Ronquist et al. 2012) with partitioned codons using variable rates and six rate categories. Two parallel runs of Markov chain Monte Carlo were performed for 5,000,000 generations, sampling every 1,000 generations. Estimated sample sizes, split frequencies, and stationarity were checked after each run. After analysis, 10% of generations were removed as burn-in and the posterior probabilities were visualized in Figtree v1.1.4 (Rambaut 2009). Two DNA-based species delimitation methods were used to determine species status. For the Assemble Species by Automatic Partitioning (ASAP) method, the Kimura (K80) Ts/Tv 2.0 model was selected and analyzed from the ASAP online platform (https://bioinfo.mnhn.fr/abi/public/asap/). A tree-based method (Poisson-Tree processes, PTP; Zhang et al. 2013) was used online using the ML tree topology. Additionally, the Automatic Barcode Gap Discovery (ABGD) method was applied using the online ABGD platform (https://bioinfo.mnhn.fr/abi/public/abgd/abgdweb.html) with default parameters, including a relative gap width (X) of 1.5 and prior intraspecific divergence (P) values ranging from 0.001 to 0.1 (Puillandre et al. 2012). The final tree was then edited using Adobe Illustrator 2024 (Adobe, San Jose, CA, USA).

 doi:10.20944/preprints202508.2023.v1

3. Results

3.1. Morphological Observations

Genus: Antithamnion

Species: Antithamnion hubbsii

Type locality: Intertidal, Pacific Grove, California, USA; (Dawson 1925)

Collection site in Korea: *Antithamnion hubbsii* collected from Sungeut beach, Gangneung-si, Gangwon-do (37°49′2.6″N, 128°53′40.5″E); collected 6 January 2024.

Habitat: Intertidal, epiphytic on other macroalgae.

Holotype: Dawson E.Y. 1925. Specimens collected from intertidal zone, Pacific Grove, California, USA; deposited in the University of California Herbarium, Berkeley (UC), accession number UC 261983.

Paratype: KNU000620-KNU000622 (Sungeut beach (37°49′2.6″N, 128°53′40.5″E), Gangneung-si, Korea, 30 March 2013, Eunyoung Shim and Soo Yeon Kim); deposited in the National Marine Biodiversity Institute of Korea (MABIK**).**

Specimens examined: KNU000620- KNU000622 (Sungeut beach (37°49′2.6″N, 128°53′40.5″E), Gangneung-si, Korea, 30 March 2013, Eunyoung Shim and Soo Yeon Kim).

GenBank accession number: PV453999 (*rbc*L), PV454032 (*psa*A)

Description : *Antithamnion hubbsii* is a delicate red alga with filamentous thallus organization displaying distinct morphological features. Thalli are generally small, reaching approximately 1-5 cm in height, with a characteristic pinnate branching pattern (Figure 1B). *Antithamnion hubbsii* is characterized by a thallus composed of both prostrate and erect axes. The erect axis comprises main and indeterminate lateral axes of unlimited growth bearing opposite pinnae of determinate growth. Indeterminate lateral axes are irregularly produced from the basal cell of pinnae in erect axes (Figure 1D).

Vegetative features: The main axis consists of prominent axial cells (Ax) that are cylindrical and elongated (Figure 1A). Branching is primarily distichous (arranged in two rows), with distinct pinnae (Pn) and pinnules (Pl) forming a regular, feather-like appearance (Figure 1A). Apical cells (AC) are prominent at the tips of growing branches and are responsible for indeterminate growth (Figure 1A). Rhizoids (rh) develop from the lower portions of the thallus and serve as attachment structures (Figure 1A). Each branch originates from a basal cell (BC) at the nodes of the main axis (Figure 1C). A distinctive feature is the presence of spherical gland cells (GC) situated adjacent to basal cells of lateral branches (Figure 1C). These gland cells are typically colorless to pale and conspicuous under light microscopy, borne on pinnae, adaxial, and covering 2 cells as shown in Table 1.

Table 1. Distinguishing characteristics of local and morphologically similar *Antithamnion* spp. as well as *Antithamnionella*.

Species	Gland cells	Indeterminae laterals	Pinnae	Branching plane	Tetrasporangia
New collection, *Antithamnion hubsii* Shim & Kim, 2024	Borne on pinnae, adaxial, covering 2 cells	Paired	Pinnate (diploid) Adaxially pectinate (haploid)	Distichous	1-cell pedicel
Antithamnion hubsii Dawson, 1963	Borne on pinnae, adaxial, covering 2 cells	Paired	Pinnate	Distichous	NA
Antithamnion nipponicum Yamada *et* Inagaki	Borne on pinnae, adaxial, covering 2 cells	Paired	Pinnate	Distichous	1-cell pedicel

 doi:10.20944/preprints202508.2023.v1

Antithamnion cruciatum Nägeli, 1847	On pinnae, covering 2 cells	Paired w/ determinate lateral	Branched decussate	Decussate	1-cell pedicel or sessile, tetrahedral
Antithamnion defectum Kylin, 1925	On pinnae, covering 2 cells	Unpaired	Branched, pectinate	Distichous	Pedicellate, undefined pedicel length
Antithamnion densum Howe, 1914	On pinnae, covering 2 cells	Paired w/ determinate lateral	Adaxially pectinate	Distichous	1-cell pedicel
Antithamnion sparsum Tokida, 1932	On pinnae, covering 2 cells	Unpaired	Adaxially pectinate	Distichous	1-cell pedicel
Antithamnionella spirographidis Wollaston, 1968	On primary branches, partly covering 1 cell	Unpaired	Simple	Distichous	Sessile

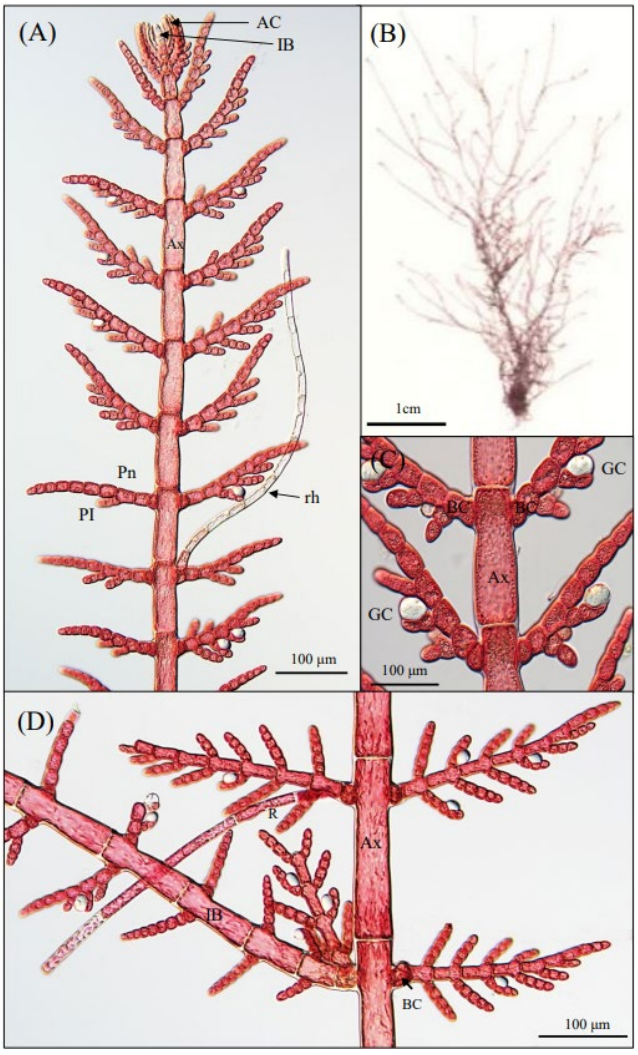

Figure 1. Morphological features of *Antithamnion hubbsii*. tetrasporophyte. Tetrasporophyte of *A. hubbsii* growing attached to intertidal rocks with distinctive bilateral branching pattern. (A) Light microscopy image showing pinnate branching pattern. AC: apical cell; IB: indeterminate branch; Pn: pinnule; PI: pinna; rh: rhizoid. Scale bar = 100 µm. (B) Higher magnification of central axis showing cellular organization. Ax: axial cell; BC: basal cell; GC: gland cell. Scale bar = 100 µm. (C) Herbarium specimen of *A. hubbsii* tetrasporophyte showing overall thallus morphology and branching pattern. Scale bar = 1 cm. (D) Close-up view of lateral branches showing the insertion of indeterminate branches (IB) and the presence of gland cells (GC) at the adaxial surface of pinnules. Note the

 doi:10.20944/preprints202508.2023.v1

repeated bilateral branching and presence of reproductive structures (R). Ax: axial cell; BC: basal cell. Scale bar = 100 μm.

Reproductive structures: The tetrasporophyte bears spherical tetrasporangia (T) that develop on specialized short branches (Figure 2A). Tetrasporangia are typically borne singly or in pairs on the adaxial side of pinnae, adjacent to gland cells (Figure 2B). Each tetrasporangium is characterized by a distinctive 1-cell pedicel structure that differentiates it from other species in the genus (Table 1). Nuclear staining reveals the presence of a single large nucleus (N) in ordinary vegetative cells (Figure 2C; white arrow). Within each tetrasporangium, nuclear staining confirmed the presence of four small nuclei (n) corresponding to the four daughter cells formed during meiotic division (Figure 2C; red arrows), confirming the typical pattern of tetrasporogenesis seen in other red algae.

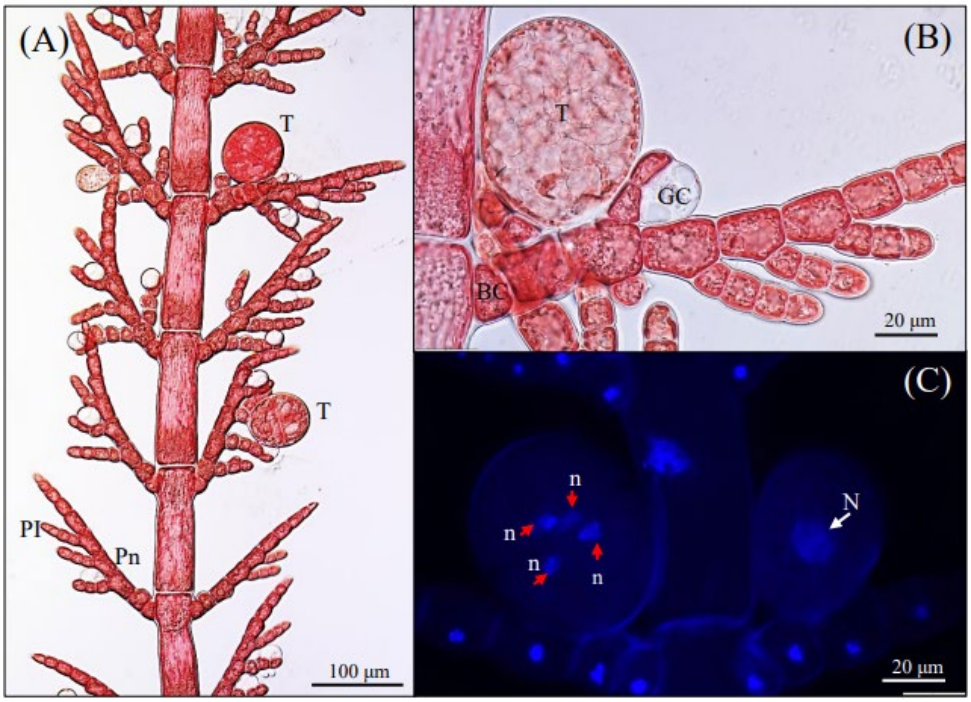

Figure 2. Tetrasporangial development in *A. hubbsii*. (A) Light microscopy image of tetrasporophyte showing mature tetrasporangia (T) distributed along the thallus. Pn: pinnule; PI: pinna. Scale bar = 100 μm. (B) Higher magnification of a mature tetrasporangium (T) showing characteristic 1-cell pedicel structure. BC: basal cell; GC: gland cell. Scale bar = 20 μm. (C) Fluorescence microscopy image of DAPI-stained tetrasporangia showing four nuclei (n) within a single tetrasporangium, confirming meiotic division. N: nucleus of vegetative cell. Scale bar = 20 μm.

Sexual dimorphism: Male and female gametophytes show distinct morphological differences (Figure 3). These reproductive structures were observed after culturing tetrasporangia for 3-6 months under laboratory conditions. Male gametophytes display dense clusters of spermatangia (arrowheads) borne on spermatangial parent cells on special branches on the adaxial side of pinnules, giving a more tufted appearance (Figure 3A,A'). Female gametophytes maintain a more regular branching pattern with procarps (arrows) developing on the basal cells of pinnae (Figure 3B). Detailed examination of the female reproductive structures reveals the development of carpogonial branch cells (CB1-3) arranged in a characteristic pattern, with the terminal carpogonium extending a trichogyne (tr) for spermatial reception (Figure 3B'). The carpogonial branch is supported by a distinct supporting cell (Su) connected to the axial cell (Ax). The branching in female gametophytes appears more orderly and pinnate compared to the clustered organization in male plants.

 doi:10.20944/preprints202508.2023.v1

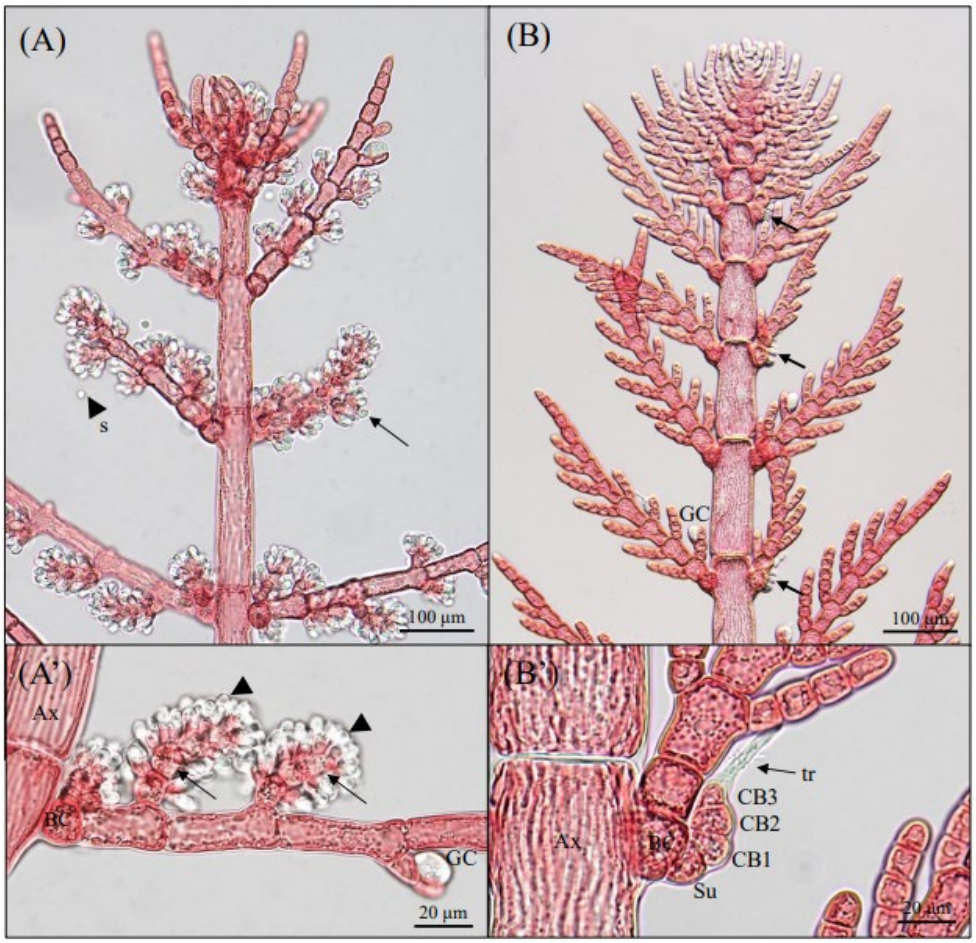

Figure 3. Morphological comparison of male and female reproductive structures in red algae *A. hubbsii*. (A) Male gametophyte showing spermatangia (arrowheads) borne on spermatangial parent cells on special branches on the adaxial side of pinnule. Ax: axial cell; BC: basal cell; sc: spermatangial cluster; GC: gland cell. (B) Female gametophyte showing upper part with procarps (arrows) borne on basal cells of pinna. Note the development of carpogonial branch cells (CB1-3) and supporting structures. Ax: axial cell; BC: basal cell; Su: supporting cell; tr: trichogyne; Au: auxiliary cell; Cp: carpogonium; Cy: cystocarp; Ft: foot cell; Fu: fusion cell; G: gonimoblast; Gi: gonimoblast initial; GI: first gonimolobes.

Carposporophyte development: The development of carposporophytes was not observed in our cultured specimens during the study period. Therefore, further investigations under controlled conditions will be required to characterize the post-fertilization stages in *A. hubbsii*.

Distinguishing characteristics: As shown in Table 1, *A. hubbsii* can be distinguished from morphologically similar species by a combination of features. It has paired indeterminate laterals, pinnate arrangement in diploid phase and adaxially pectinate in haploid phase, and distichous branching plane. These characteristics, together with the distinctive gland cell arrangement and 1-cell pedicel of tetrasporangia, clearly differentiate *A. hubbsii* from other related species such as *A. nipponicum*, *A. cruciatum*, and *A. defectum*. While *A. hubbsii* shares some features with *A. nipponicum*, such as paired indeterminate laterals and distichous branching, our molecular analyses demonstrate that they represent distinct species.

This combination of morphological features, particularly the arrangement of pinnae, location of gland cells, and pattern of tetrasporangia development, supports the identification of this specimen as *Antithamnion hubbsii*, consistent with its phylogenetic placement shown in the molecular analyses.

 doi:10.20944/preprints202508.2023.v1

3.2. Phylogenetic Analyses

The 1467 base pairs (bp) of *rbc*L and 1523 bp of *psa*A were sequenced from samples collected in Korea. The phylogenetic trees were constructed by aligning the newly generated sequences with those downloaded from GenBank (Table 2, Figure 4).

Table 2. Collections of *Antithamnion* and outgroup taxa from which *rbc*L and *psa*A were obtained.

Species	Location of collection and/or source of culture; collector or depositor	Date	GeneBank Accession NO.
ribulose-1,5-bisphosphate carboxylase/oxygenase large subunit (rbcL) gene			
Antithamnion aglandum Kim *et* Lee	Jeoongdori, Wando, South Korea; S.M. Boo, T.O. Cho & H.G. Choi	29.01.1999	AY594700
Antithamnion cruciatum	Mulroy Bay, Co. Donegal, Ireland; C.A. Maggs	16.02.1993	JN089394
Antithamnion defectum	Sitka, AK, USA	21.06.2005	GO252484
Antithamnion defectum	California, La Jolla, USA; C.A. Maggs	27.07.1995	JN089391
Antithamnion defectum	Skellig Rocks, Co. Kerry Ireland; C.A. Maggs	01.06.1992	JN089395
Antithamnion hanovioides (Sonder) De Toni	Pennington Bay, Kangaroo Island, S. Australia; T.O. Cho & B.Y. Won	07.09.1995	AY591927
Antithamnion hubbsii	Spain	07.05.2019	MK814610
Antithamnion hubbsii Shim *et* Kim	Sungeut beach, Gangwon-do, South Korea; E. Shim, S.Y. Kim & G.H. Kim	06.01.2024	PV453999
Antithamnion kylinii	Canada		JN089393
Antithamnion nipponicum Yamada *et* Inagaki	Hachinohe, Aomori, Japan; M. Kamiya	21.05.1995	AY594699
Antithamnion nipponicum NC-1	In front of Duke University Marine Laboratory, Pivers I, Beaufort, Carteret Co., North Carolina, USA; T.O. Cho & B.Y. Won	29.10.2003	AY591928
Antithamnion nipponicum	Maengbang, Samcheok, South Korea; E.C. Yang & S.M. Boo	2016	AY295174
Antithamnion nipponicum CA	Halfmoon Bay, California, USA; T.O. Cho & B.Y. Won		AY591930
Antithamnion nipponicum	Aragami, Funakoshi, Yamada, Japan; Masahiro Suzuki	29.08.2014	LC821146
Antithamnion pectinatum (Montagne) Brauner	Lee Bay, Stewart Island, New Zealand; W.A. Nelson	03.10.2004	DQ023481
Antithamnion pectinatum	Kenton On Sea, South Africa; Faith Mshiywa	24.11.2017	OR939842
Antithamnion sp.	Mallacoota, VIC, Australia; H. Verbruggen & K. Dixon	2019	MK125356
Antithamnion sp.	Ewing Bank, Offshore Louisiana, USA;	29.05.2011	KY994130

 doi:10.20944/preprints202508.2023.v1

J.Richards

Antithamnion sparsum Tokida	Nova Sotia, Canada	2021	OP600459
Antithamnion sparsum	Daechon, South Korea; H.G. Cho	23.04.1992	JN089392
Antithamnion ternifolia (Hooker *et* Harvey) Lyle	Williamston, Australia; J. West	28.05.2002	AY591926
Amoenothamnion planktonicum	WestAP, Australia		OR359632
Antithamnionella miharai	Youngeumjun, Sokcho, South Korea	09.05.2006	GQ252485
Antithamnionella spirographidis	Monterey Bay, California, USA; T.O. Cho	11.12.1999	AY591923
Photosystem I P700 apoprotein (psa*A*)			
Aglaothamnion callophyllidicola	Kamo Bay, Oki Island, Japan; E.C. Yang & S.M. Boo	07.05.2003	DQ787601
Aglaothamnion hookeri	Castilo San Cristobal, Canary, Spain	24.04.2004	EU195020
	Antithamnion hubbsii		MK814610
Antithamnion hubbsii Shim *et* Kim	Sungeut beach, Gangwon-do, South Korea; E. Shim, S.Y. Kim & G.H. Kim	06.01.2024	PV454032
Antithamnion nipponicum	-	2019	AY295136
Antithamnionella sp.	Choshi, Chiba, Japan; E.C. Yang & S.M. Boo	27.07.2002	DQ787600
Antithamnionella ternifolia	-	2019	MK814608
Campylaephora kondoi	Hakampo, Taean, South Korea; E.C. Yang & S.M. Boo	2003	AY295138
Corallina pilulifera	Nagasaki, Choshi, Chiba, Japan; E.C. Yang & S.M. Boo	01.08.2004	DQ787594

Molecular phylogenetic analyses based on both *rbc*L (Figure 4A) and *psa*A (Figure 4B) sequences revealed that specimens collected from Sungeut Beach in Gangneung, South Korea formed a well-supported clade with previously reported *Antithamnion hubbsii*. In the *rbc*L phylogeny, our Korean *A. hubbsii* (PV453999) formed a strongly supported clade with *A. hubbsii* from California (AY591930) with bootstrap values of 98/99 for ML/Bayesian analyses. This clade was sister to *A. nipponicum* sequences with minimal genetic distance (0.25-0.29%). The *psa*A gene analysis similarly grouped our Korean *A. hubbsii* specimen (PV454032) with previously reported *A. hubbsii* (MK814610) with high statistical support (99.4/100), forming a sister relationship to *A. nipponicum* (AY295136) with only 0.34% genetic distance.

Both genes consistently placed the newly reported Korean specimens within the *A. hubbsii* lineage, distinct from but closely related to *A. nipponicum*. The ASAP and PTP analyses confirmed the species delimitation, specifically highlighting the distinct status of *A. hubbsii* from Sungeut Beach in Gangwon-do, South Korea. This represents the first report of *A. hubbsii* in Korean waters, as previous records of this species were primarily from the United States.

 doi:10.20944/preprints202508.2023.v1

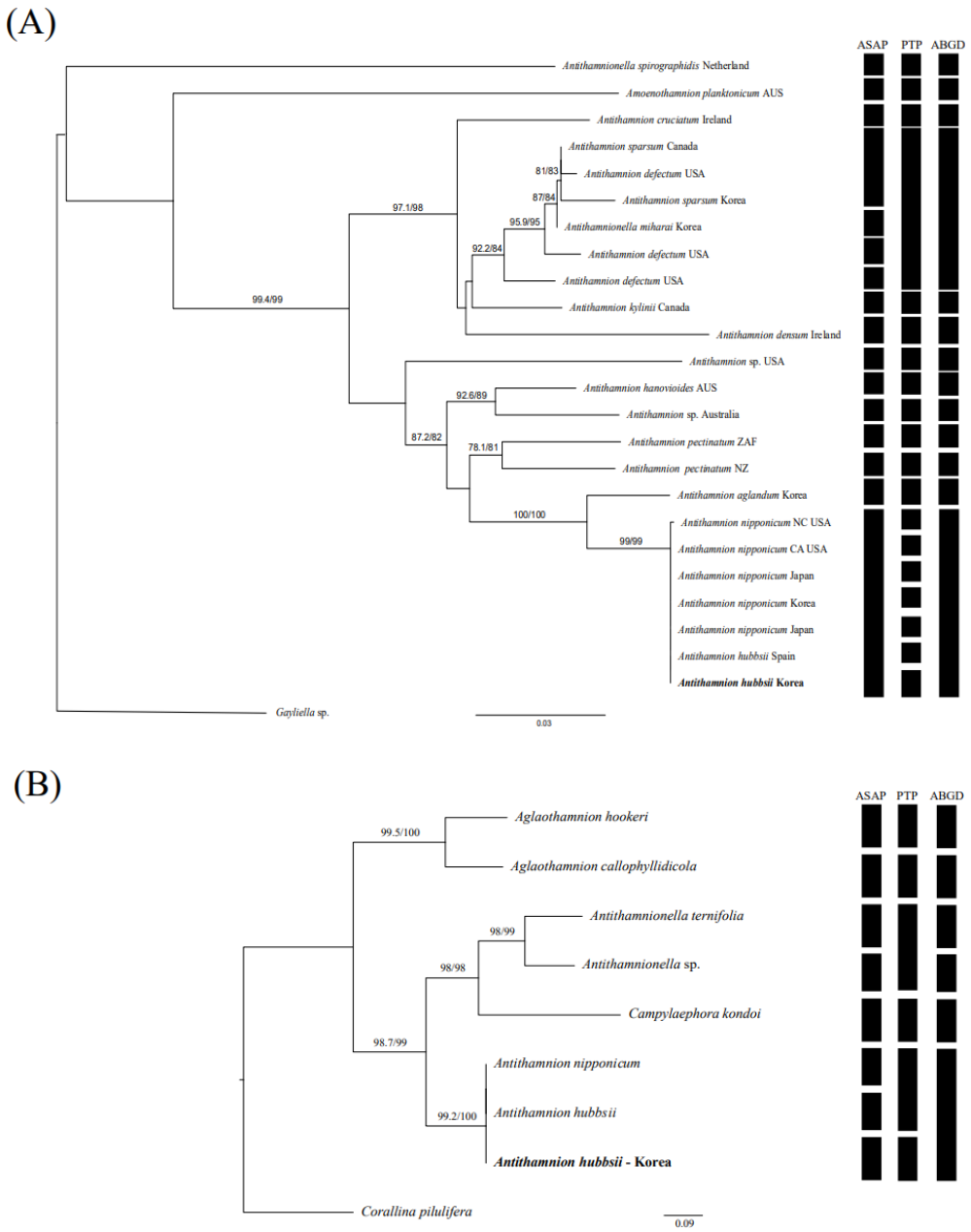

Figure 4. Maximum Likelihood (ML) phylogenetic trees of *Antithamnion* species based on (A) *rbc*L and (B) *psa*A gene sequences. Numbers at nodes indicate bootstrap support values (%) for ML analysis. The trees were rooted using *Cystoclonium purpureum* and *Ceramium piluliferoides* as outgroups for *rbc*L and psaA, respectively. Newly sequenced *A. hubbsii* specimens from Korea are indicated in bold. The matrices to the right of each tree summarize species delimitation results based on three methods: ASAP (Assemble Species by Automatic Partitioning), PTP (Poisson Tree Processes), and ABGD (Automatic Barcode Gap Discovery). Black squares indicate groups recognized as separate species by each method. Conflicting results between ASAP and PTP analyses highlight the taxonomic uncertainty between *A. hubbsii* and *A. nipponicum*.

4. Discussion

The present study documents the first confirmed occurrence of *Antithamnion hubbsii* in Korean waters, based on both detailed morphological characteristics and molecular phylogenetic evidence. The species has likely been misidentified as *A. nipponicum* in previous surveys due to their striking morphological similarities. This finding highlights the taxonomic complexity within the genus *Antithamnion* and emphasizes the importance of integrating molecular tools with traditional morphological approaches for accurate species identification in red algae (Saunders, 2005; Freshwater et al., 2010).

 doi:10.20944/preprints202508.2023.v1

The taxonomic history of *Antithamnion* species has been marked by numerous revisions and reclassifications over the past century. The genus was first established by Nägeli (1847) and has since undergone significant taxonomic refinement. Our findings contribute to this ongoing taxonomic discourse by providing molecular evidence for the presence of *A. hubbsii* in Korean waters. The extremely close genetic relationship between *A. hubbsii* and *A. nipponicum* revealed in our analyses (0.25-0.29% divergence in *rbc*L and 0.34% in *psa*A) reinforces the taxonomic challenges within this genus. While Cho et al. (2007) previously suggested these taxa might represent the same species based on minimal genetic differences, our ASAP analysis results support their distinction as separate species despite these minimal differences. This conclusion contradicts our PTP analysis results, which grouped them as a single species, reflecting the ongoing methodological challenges in delimiting species boundaries within closely related red algal taxa (Payo et al., 2013; Leliaert et al., 2014).

Although the origin of *A. hubbsii* in Korean waters remains uncertain, its presence calls for a re-assessment of regional red algal biodiversity, particularly in taxa with cryptic or morphologically similar species. Previous studies have shown that minimal genetic divergence can mask true taxonomic identity, highlighting the necessity for refined field sampling and the application of multi-locus molecular approaches (Steen & Scrosati, 2004; Freshwater et al., 2010).

At present, it remains unclear whether *A. hubbsii* is native to Korean waters or introduced. Regardless of its origin, its presence calls for a re-evaluation of red algal biodiversity in the region, particularly within genera that include cryptic or morphologically similar species. Previous studies have emphasized that even minimal genetic differences can obscure true taxonomic boundaries in red algae (Saunders, 2005; Payo et al., 2013). Future studies should aim to resolve these uncertainties through expanded field surveys and more refined molecular analyses (Steen & Scrosati, 2004; Freshwater et al., 2010).

These taxonomic challenges are not only of academic interest but also have important implications for biodiversity monitoring and non-native species management. Accurate identification of *A. hubbsii* contributes to our understanding of species diversity in Korean coastal ecosystems and may aid in improving detection of potential introductions. Given the morphological and genetic ambiguity between *A. hubbsii* and *A. nipponicum*, clarifying their taxonomic relationship is crucial (Leliaert et al., 2014; Olenin et al., 2011). A systematic re-evaluation of the genus *Antithamnion* will be essential to establish robust species boundaries, which in turn can inform ecological research and conservation strategies (Williams & Smith, 2007).

Acknowledgement: This work was supported by the management of Marine and Fishery Bio-resources Center (2025) funded by the National Marine Biodiversity Institute of Korea (MABIK) and Korea Institute of Marine Science & Technology Promotion(KIMST) funded by the Ministry of Oceans and Fisheries, Korea(RS-2025-02303933) and the National Research Foundation of Korea (NRF) grant funded by the Korea government (MSIT) (NRF-2022R1A2C1091633).

References

Athanasiadis A and Tittley I. 1994. Antithamnioid algae (Rhodophyta, Ceramiaceae) newly recorded from the Azores. *Phycologia* 33, 77-80

Brooks CM and Krumhansl K. 2023. First record of the Asian *Antithamnion sparsum* Tokida, 1932 (Ceramiales, Rhodophyta) in Nova Scotia, Canada. *BioInvasions Records* 12:745-752.

Carlton JT and Geller JB. 1993. Ecological roulette: The global transport of nonindigenous marine organisms. *Science* 261:78-82.

Chernomor O, von Haeseler A and Minh BQ. 2016. Terrace aware data structure for phylogenomic inference from supermatrices. *Systematic Biology* 65:997-1008.

Cho TO, Boo SM, Hommersand MH, Maggs CA, McIvor L and Fredericq S. 2005. *Gayliella* gen. nov. in the tribe Ceramieae (Ceramiaceae, Rhodophyta) based on molecular and morphological evidence. *Journal of Phycology* 41:726-738.

 doi:10.20944/preprints202508.2023.v1

Cho TO, Won BY and Fredericq S. 2007. *Antithamnion nipponicum* (Ceramiaceae, Rhodophyta), incorrectly known as *A. pectinatum* in western Europe, is a recent introduction along the North Carolina and Pacific coasts of North America. *European Journal of Phycology* 40:323-335.

Dawson EY. 1925. Studies of intertidal algae at Pacific Grove, California. *Bulletin of the California Academy of Sciences* 24:31-59.

Felsenstein J. 1985. Confidence limits on phylogenies: An approach using the bootstrap. *Evolution* 39:783-791.

Freshwater DW, Tudor K, O'Shaughnessy K and Wysor B. 2010. DNA barcoding in the red algal order Gelidiales: Comparison of COI with *rbc*L and verification of the "barcoding gap". *Cryptogamie, Algologie* 31:435-449.

Hommersand MH, Freshwater DW, Lopez-Bautista JM and Fredericq S. 2009. Proposal of the Euptiloteae Hommersand et Fredericq, trib. nov. and transfer of some southern hemisphere Ptiloteae to the Callithamnieae (Ceramiaceae, Rhodophyta). *Journal of Phycology* 45:1065-1080.

Kalyaanamoorthy S, Minh BQ, Wong TKF, von Haeseler A and Jermiin LS. 2017. ModelFinder: Fast model selection for accurate phylogenetic estimates. *Nature Methods* 14:587-589.

Kang JH, Jang JE, Kim JH and Kim MS. 2020. DNA barcoding of the genus *Grateloupia* (Rhodophyta) from Korea: An assessment of DNA barcoding markers for species identification. *Diversity* 12:3.

Klochkova TA, Kang SH, Cho GY, Pueschel CM, West JA and Kim GH. 2006. Biology of a terrestrial green alga, *Chlorococcum* sp. (Chlorococcales, Chlorophyta), collected from the Miruksazi stupa in Korea. *Phycologia* 45:349-358.

Leliaert F, Verbruggen H, Vanormelingen P, Steen F, López-Bautista JM, Zuccarello GC and De Clerck O. 2014. DNA-based species delimitation in algae. *European Journal of Phycology* 49:179-196.

Minh BQ, Schmidt HA, Chernomor O, Schrempf D, Woodhams MD, von Haeseler A and Lanfear R. 2020. IQ-TREE 2: New models and efficient methods for phylogenetic inference in the genomic era. *Molecular Biology and Evolution* 37:1530-1534.

Nägeli C. 1847. Die neueren Algensysteme und Versuch zur Begründung eines eigenen Systems der Algen und Florideen. *Neue Denkschriften der Allgemeinen Schweizerischen Gesellschaft für die Gesammten Naturwissenschaften* 9:1-275.

Olenin S, Alemany F, Cardoso AC, Gollasch S, Goulletquer P, Lehtiniemi M, McCollin T, Minchin D, Miossec L, Occhipinti-Ambrogi A, Ojaveer H, Jensen KR, Stankiewicz M, Wallentinus I and Aleksandrov B. 2011. Marine Strategy Framework Directive – Task Group 2 Report: Non-indigenous species. Luxembourg: Office for Official Publications of the European Communities.

Payo DA, Leliaert F, Verbruggen H, D'hondt S, Calumpong HP and De Clerck O. 2013. Extensive cryptic species diversity and fine-scale endemism in the marine red alga *Portieria* in the Philippines. *Proceedings of the Royal Society B: Biological Sciences* 280:20122660.

Puillandre N, Lambert A, Brouillet S and Achaz G. 2012. ABGD, Automatic Barcode Gap Discovery for primary species delimitation. *Molecular Ecology* 21:1864-1877.

Rueness J, Heggøy E, Husa V and Sjøtun K. 2007. First report of the Japanese red alga *Antithamnion nipponicum* on the west coast of Norway. *Aquatic Invasions* 2:431-434.

Williams SL and Smith JE. 2007. A global review of the distribution, taxonomy, and impacts of introduced seaweeds. *Annual Review of Ecology, Evolution, and Systematics* 38:327-359.

Yoon HS, Hackett JD and Bhattacharya D. 2002. A single origin of the peridinin- and fucoxanthin-containing plastids in dinoflagellates through tertiary endosymbiosis. *Proceedings of the National Academy of Sciences* 99:11724-11729.

Zhang J, Kapli P, Pavlidis P and Stamatakis A. 2013. A general species delimitation method with applications to phylogenetic placements. *Bioinformatics* 29:2869-2876.

Zuccarello GC, Burger G, West JA and King RJ. 1999. A mitochondrial marker for red algal intraspecific relationships. *Molecular Ecology* 8:1443-1447.